Preparation and characterization of two types of separate collagen nanofibers with different widths using aqueous counter collision as a gentle top-down process

2014 Mater. Res. Express 1 045016

(http://iopscience.iop.org/2053-1591/1/4/045016)

Materials Research
Express

Preparation and characterization of two types of separate collagen nanofibers with different widths using aqueous counter collision as a gentle top-down process

Tetsuo Kondo[1], **Daisuke Kumon**[1], **Akiko Mieno**[1], **Yutaro Tsujita**[1] and **Ryota Kose**[2]

[1] Graduate School of Bioresource and Bioenvironmental Sciences, Kyushu University, 6-10-1 Hakozaki, Higashi, Fukuoka 812-8581, Japan
[2] Faculty of Agriculture, Tokyo University of Agriculture and Technology, 3-5-8 Saiwai-cho, Fuchu, Tokyo 183-8509, Japan
E-mail: tekondo@agr.kyushu-u.ac.jp

Received 30 August 2014
Accepted for publication 16 September 2014
Published 22 October 2014

Materials Research Express **1** (2014) 045016

doi:10.1088/2053-1591/1/4/045016

Abstract

Two types of single collagen nanofibers with different widths were successfully prepared from native collagen fibrils using aqueous counter collision (ACC) as a top-down process. A mild collision of an aqueous suspension at a 100 MPa ejection pressure yielded nanofibers, termed CNF100, which have an inherent axial periodicity and are ~100 nm in width and ~10 μm in length. In contrast, ACC treatment at 200 MPa provided a non-periodic, shorter and thinner nanofiber, termed CNF10, that was ~10 nm in width and ~5 μm in length. Both nanofibers exhibited the inherent triple helix conformation of native collagen supramolecules. Even a medial collision that exceeded the above ACC pressures provided solely a mixture of the two nanofiber products. The two nanofiber types were well characterized, and their tensile strengths were estimated based on their sonication-induced fragmentation behaviors that related to their individual fiber morphologies. As a result, CNF10, which was found to be a critical minimum nanofibril unit, and CNF10 exhibited totally different features in sizes, morphology, tensile strength and viscoelastic properties. In particular, as the mechanical strength of the molecular scaffold affects cell differentiation, the two collagen nanofibers prepared here by ACC have the potential for controlling cell differentiation in possibly different ways, as they have different mechanical properties. This encourages the consideration of the application of CNF100 and CNF10 in the fabrication of new functional materials with unique properties such as a scaffold for tissue engineering.

Keywords: collagen, nanofiber, tensile strength, morphology, structure-property relationship, nano building block

1. Introduction

In nature, hierarchical structures within biomacromolecules, such as collagen, chitin and cellulose, are built up from the molecular level through the nanometer scale to nano/micrometer scales. Collagen molecules, which consist of three helical polypeptide chains and establish a unique hierarchical structure, are the most abundant biomacromolecules in animal tissues. A collagen fibril in an extracellular matrix is synthesized as a long fibrous structure with the arrangement of the triple helical polypeptide units aligned in both longitudinal and oblique directions and is further assembled with other fibers to produce a unique three-dimensional fiber structure. A collagen fiber is comprised of a bundle of collagen fibrils 10–300 nm in width as building blocks. The right-handed, triple helical structure of a collagen molecule, which consists of three left-handed helical polypeptide chains, is arranged regularly in both the longitudinal and lateral directions in a collagen fibril. Such an arrangement of collagen molecules forms the unique periodic-banding morphology of the collagen fibril (figure 1) [1–8].

Collagen supramolecules or tropocollagen consist of three helical polypeptide chains with a repeating Gly-X-Y amino acyl residue pattern, where the *X* and *Y* positions are often proline and hydroxyproline, respectively [3, 4]. They are organized together to form a triple helical structure ~1.5 nm in width and ~300 nm in length. This triple helix is the minimum building block in the hierarchical structure of a collagen fibril, and five supramolecules assemble to form a collagen microfibril [5, 6]. Microfibrils are finally arranged with a specific staggered pattern in both the fibril's longitudinal and lateral directions and are stabilized by intermolecular hydrogen bonds, electrostatic interactions and chemical crosslinks [7, 8]. Such a systematic arrangement of collagen molecules exhibit a specific typical periodic-banding morphology of the collagen fibril in transmission electron micrographs (TEM) [9, 10].

The relationships between the hierarchical structure of collagenous tissue and its mechanical properties have been investigated at the micrometer scale. Namely, the strength of a collagen fiber has been reported to depend on the fiber diameter, which is in a relationship between the hierarchical structure and mechanical properties [2, 11, 12]. In previous studies, the self-assembly of collagen molecules, which is water-solubilized collagen prepared by acid or alkali treatment, and gelatin obtained by heating the collagen molecules have been mainly employed for targeting products [13–15]. However, to our knowledge, there has been no research to date that has focused at the nanometer scale, presumably because there has been no established method to extract collagen nanofibers from native fibers in a top-down manner. Therefore, the production and study of a collagen nano-building block that includes collagen nanofibers would provide valuable insight into important features or properties of collagen. In particular, it was expected here that the formation process and the strength of a collagen hydrogel formed from a collagen nanofiber network that includes large amounts of water clusters would be very different from conventional results.

Recently, Kondo *et al* proposed a method for preparing separate cellulose nanofibers (so-called nanocellulose) as a dispersion in water using aqueous counter collision (ACC) to process the three-dimensional networks of fibers found in microbial cellulose pellicles. This technique allows biobased materials and carbons to be processed into nano-objects using only a pair of

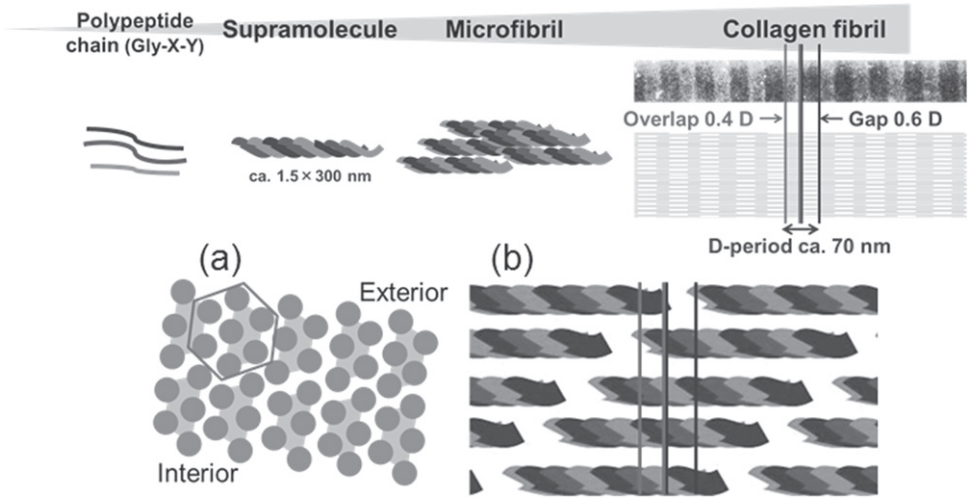

Figure 1. Schematic illustrations of a sequence of hierarchical assemblies of collagen molecules to collagen fibril (upper image). The bottom images indicate (a) cross-sectional and (b) longitudinal schematic illustrations of collagen fibrils [1–8].

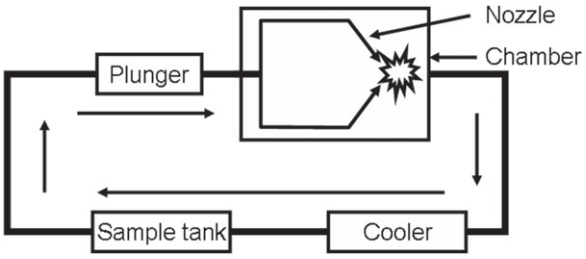

Figure 2. Aqueous counter collision system using a pair of water jets [16–21].

water jets, without the need for any chemical modifications [16–21]. Basically, ACC reduces biomaterials to nanoscale objects using the collision energy of dual water jets. This strategy is capable of overcoming van der Waals forces and hydrogen bonds in the absence of chemical modification. Thus, ACC is one of the gentlest, mildest methods available among the top-down reducing processes. This system involves an aqueous suspension of μm-sized sample particles divided between two nozzles that face each other (figure 2). The opposing ejected suspensions collide at a high speed, resulting in nano-pulverization of the dispersed sample. The obtained material can be homogeneously reduced and further reduced in size by repeated collisions or increased ejection pressure. In the current study, ACC was applied to hydrophobic carbons, such as fullerene (C_{60}), multiwalled carbon nanotubes and graphite, to successfully prepare aqueous suspensions [21].

Furthermore, ACC can selectively cleave particular interactions in soft materials, such as polysaccharides, proteins and nucleic acids, by controlling the number of collisions and/or the ejection pressure. In this study, the goal was to use ACC to extract nano-building blocks from native collagen fibers. Considering the fiber's unique structure, three disassembly patterns were assumed for reducing collagen fibers to nanoscale objects: 1) cleavage of longitudinal interfacial interactions, 2) cleavage of both longitudinal and lateral interfacial interactions and 3) cleavage of intramolecular interactions in the collagen triple helix. Thus, the goal of this

study was to understand how collagen fibers were reduced by ACC to nanofibers as well as to illuminate how the hierarchical structures relate to measured mechanical properties at each size-scale.

2. Materials and methods

2.1. ACC treatment of collagen fibers

Collagen fibers from bovine skin type I collagen fibrils were provided from Nippi Inc. (Tokyo, Japan). Collagen fibers (0.01% by wt) were dispersed in deionized water with stirring for 1 d at room temperature prior to homogenization at 10 000 or 20 000 rpm for 3 min using a homogenizer (Physcotron NS-51, Microtec Co., Ltd, Chiba, Japan). In general, collagen molecule self-assembly is performed in the 5–8 pH range [11], while an acid-solubilized collagen is prepared in 2–3 pH [11, 22]. Here, the initial pH value for the collagen fiber suspension before ACC treatment was 4, which was appropriate to maintain the morphology and dispersion state of the collagen sample. Aqueous suspensions were subjected to ACC treatment (figure 2, Sugino Co., Toyama, Japan) under 100, 120, 150, 180, 190 and 200 MPa of nozzle ejection pressure in combination with 10, 30, 60 and 90 cycle repetition times (or Pass) [16–21]. The number of collisions and the collision pressure were critical factors in tailoring the properties of the resulting nanofibers. The nozzle diameter was 160 μm, with the jets' collision angle typically set at ~170 degrees. A single collision of the jets simultaneously generates heat such that a 50 °C temperature increase is associated with a pressure of 200 MPa [17], which is the maximum ejection pressure employed in this study. Because of this heat generation, a cooling system based on a flow of water was applied immediately downstream from the jet-collision zone in the chamber.

2.2. Measurements

2.2.1. TEM observation. An aqueous suspension containing 0.01% ACC-treated collagen fibers (by wt) was mounted on a copper grid. An aqueous 0.25% surfactant solution was next applied to the grid, followed by negative staining with aqueous 1% uranyl acetate. The specimen was then washed thoroughly with deionized water before a second application of the negative stain; finally, the specimen was air-dried. A TEM observation was carried out with a JEM-1010 (JEOL Ltd, Tokyo, Japan) operated at 80 kV of accelerating voltage with a beam current of <70 μA. The TEM images were acquired at magnifications from 300 k to 150 k in the negative films. The images were scanned for digitization and for measurement of the widths and lengths of the >100 individual collagen nanofibers using Image-Pro Plus software version 4.1 (Media Cybernetics, Inc., Rockville, MD, USA).

2.2.2. Circular dichroic (CD) spectroscopy. The specimens for the CD measurements were prepared according to the following procedure: An aqueous suspension containing 0.15% of collagen fibers (by wt) was stirred for 1 d, followed by the addition of NaCl to a final 10% concentration (by wt). The dispersion was then centrifuged at 10 °C under 1.0×10^4 g for 20 min using a high-speed refrigerated microcentrifuge (MX-301, Tomy Seiko Co., Ltd, Tokyo, Japan). After the precipitate was dialyzed in deionized water, 0.01% dispersions (by wt) were treated by ACC using 100 or 200 MPa ejection pressure with 10, 30, 60 or 90 Pass.

Dispersed samples in the water prepared as above were provided for CD spectroscopic measurements using a JASCO J-820 spectrometer (JASCO International Co., Ltd, Tokyo, Japan). The CD spectra were measured at wavelengths from 183 to 300 nm under a temperature of 15 °C. The sample cell length for longer (210–300 nm) and shorter wavelengths (183–300 nm) was 10 and 1 mm, respectively. The scanning rate was 50 nm min^{-1} at a 1 nm resolution, and the response time was set at 2 s.

2.2.3. Sonication-induced fragmentation. Each aqueous dispersion of separated collagen nanofibers was sonicated using a UD-200 sonicator (Tomy Seiko Co., Ltd) at 200 W maximum power and 20 kHz operating at 10% output power. Ultrasonic waves were applied in 20 min on 5 min off cycles for up to 360 min. The dispersions temperature was maintained at ~8 °C in an ice water bath.

2.2.4. Viscoelastic measurements. For dynamic viscoelastic measurements, specimens were prepared in the following manner: collagen fibers (0.8% by wt) were dispersed in deionized water and stirring for 1 d prior to ACC treatment under either 100 or 200 MPa ejection pressure with 30 Pass. The resulting samples were held in a refrigerator for 2 d.

Dispersed samples in water prepared as above were analyzed with a cone-plate type rheometer (Rheosol-G2000, UBM Co., Ltd, Kyoto, Japan). The radius of both the cone and plate was 50 mm, and the cone angle was 28 degrees. The rheometer was equipped with a reservoir to prevent sample-drying during measurements. Dynamic viscoelastic measurements were performed at 5 ± 0.1 °C and with measured frequencies ranging from 0.05 to 56 rad s^{-1}. The dynamic strain amplitude (γ) was 0.208 (10%).

3. Results and discussion

3.1. Preparation of collagen nanofibers by ACC

Prior to ACC treatment, the size and morphology on the initial collagen fibers to be disintegrated in a homogenizer were estimated by TEM observation. The initial collagen fibers were a few micrometers in width and were composed of fibrils with an inherent periodic banding (periodicity, 64 ± 2 nm) 110–130 nm in width (figure 3, upper left image).

Collagen fibers and fibrils were first subjected to ACC at two typically extreme ejection pressures: 100 and 200 MPa. The two upper-right images in figure 3 show TEM images of separate collagen nanofibers prepared by ACC with 30 Pass. The morphology and size of collagen nanofibers after ACC treatment appeared remarkably different, depending on the ejection pressure. An ACC treatment at 100 MPa produced single collagen nanofibers with a periodic-banding structure ~100 nm in width and ~10 μm in length; these nanofibers are called CNF100. The periodic banding exhibited a periodicity of 64 ± 2 nm, which is the same as the initial collagen fibers. Conversely, ACC treatment at 200 MPa produced single collagen nanofibers with a non-periodic and smaller (shorter and thinner) size of ~10 nm in width and ~5 μm in length; these nanofibers are called CNF10. As a result, ACC treatment at 200 MPa reduced both the width and length of the initial collagen fibers, while treatment at the lower pressure decreased only the collagen fibril lengths.

When the collagen fibers and fibrils were subjected to ACC treatment at various ejection pressures ranging from 100 to 200 MPa, the resulting collagen nanofibers were typically a

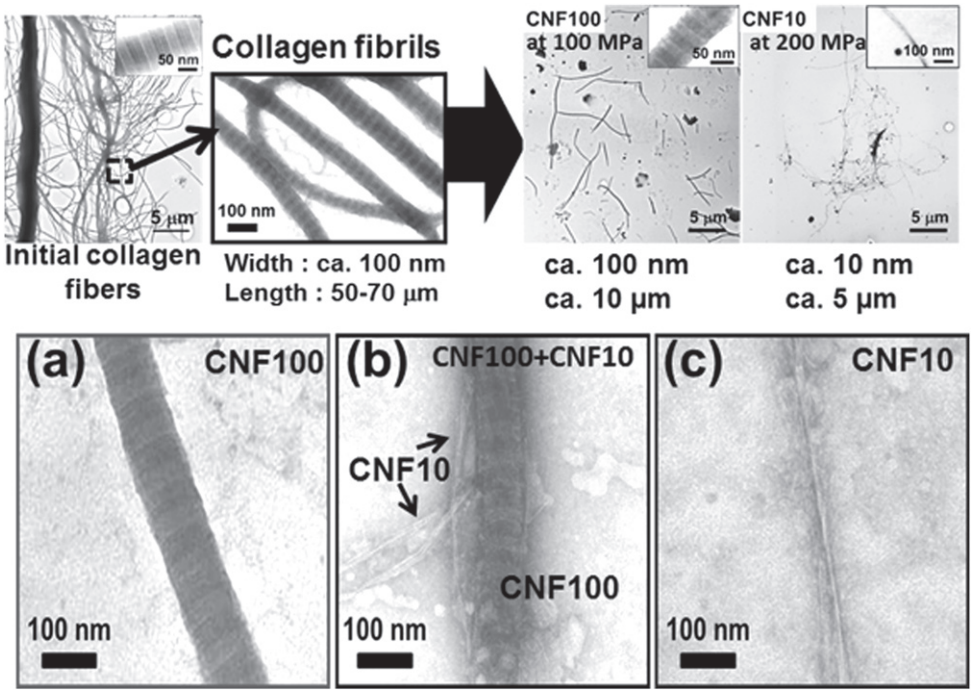

Figure 3. TEM images of collagen fibers before (a) and after ACC treatment (upper images) and TEM micrographs of separate collagen nanofibers (CNF100 with a width of ~100 nm and CNF10 with a width of ~10 nm) prepared by ACC under different ejection pressures of ((a)–(c)) 100, 150 and 200 MPa, respectively.

mixture of the two types: CNF100 and CNF10, without a gradient change in fiber width related to the ACC ejection pressure. Specifically, the sizes and morphology of the collagen nanofibers did not change—except for the proportions of CNF100 and CNF10—in a manner dependent on the ACC ejection pressure. It was noted that ACC treatments with pressures from 120 to 150 MPa (figure 4; the dotted areas are indicated by the arrow) produced a mixture of CNF100 and CNF10 collagen nanofibers. Figures 3(a)–(c) show the resulting nanofibers of CNF100 alone, which is a mixture of the two types, and of CNF10 alone after ACC treatments at 100, 150 and 200 MPa, respectively. The CNF100 product's inherent periodic banding in the TEM imaging was still observed in the mixtures after ACC treatment at ejection pressures ranging from 100 to 150 MPa (figures 3(a) and (b) and figure 4). The width of the collagen nanofibers was 100–115 nm, confirming that they were CNF100. Then, collagen nanofibers without periodic banding in TEM began to be observed in the mixtures along with CNF100 at the higher pressures. Over an ejection pressure of 150 MPa, the CNF100 disappeared significantly (figure 4(a)), and only CNF10 remained in the ACC-treated dispersions (figures 4(b) and (c)). The ACC treatment appeared to peel off of the CNF10, which was 10 nm in width, from the CNF100's surface to produce the resulting aqueous suspension. These results indicated that there might be a critical energy range for these intermolecular engagements and that a suitable ejection pressure can thereby selectively cleave specific intermolecular interactions (figure 6; interactions to be described below).

Table 1 lists changes in both the width and length for the collagen nanofibers CNF100 and CNF10, depending on the Pass numbers at the ACC ejection pressures of 100 and 200 MPa.

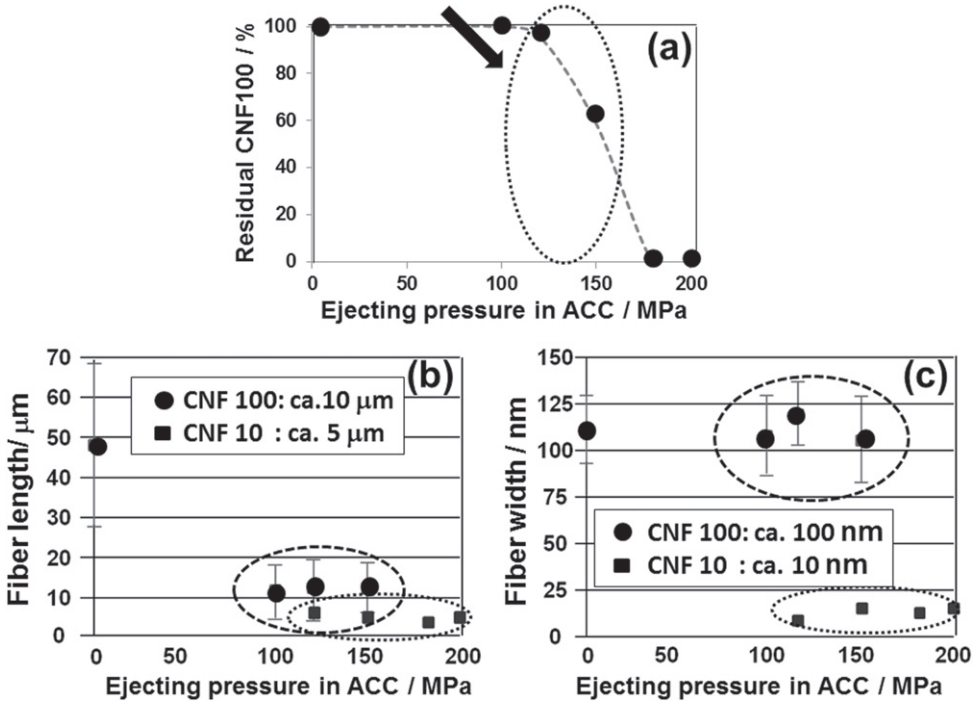

Figure 4. Change of the collagen fiber length (b) and width, (c) together with changes in the amounts of residual CNF100 (a) after the ACC treatment at various ejection pressures from 100 to 200 MPa.

Table 1. Dependence of width and length of the collagen nanofibers on the Pass numbers, prepared by ACC treatment using ejection pressures of 100 and 200 MPa.

Ejecting pressure/MPa—Pass	Width/nm	Length/μm
100, 200 – 0	112 ± 17	[a]48 ± 21
100 – 30	109 ± 22	11 ± 7
100 – 60	112 ± 20	12 ± 8
100 – 90	104 ± 23	11 ± 7
200 – 10	13 ± 2	4 ± 2
200 – 30	12 ± 4	5 ± 2
200 – 60	13 ± 3	4 ± 2
200 – 90	12 ± 2	5 ± 1

[a] Distribution of length of the initial collagen fibers is relatively large to be measured.

Both measurement values did not change significantly, even with the increasing Pass number. For CNF10 at 200 MPa, the width became one tenth of the initial collagen fibril and one tenth of the CNF100 widths, whereas the length of CNF10 corresponded to half of CNF100's length. Thus, when a dual ACC method was employed that included consecutive collisions with these two different ejection pressures, it produced novel, shorter and/or thinner collagen nanorods, a description of which will appear in a future paper.

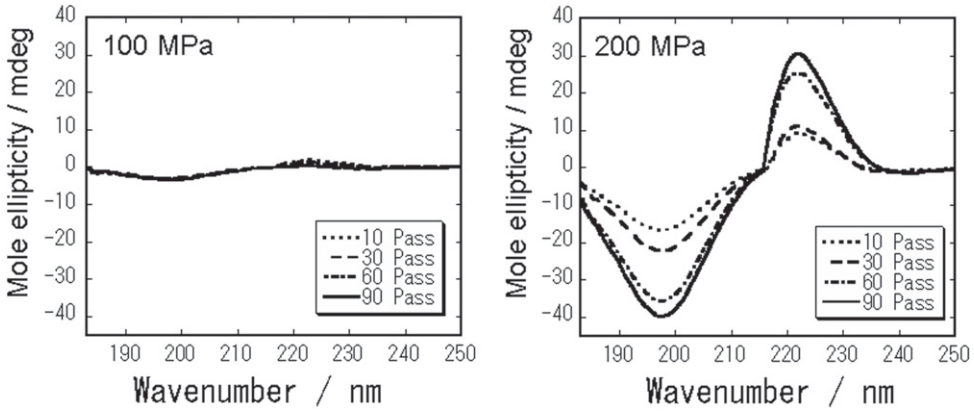

Figure 5. CD spectra of collagen nanofiber dispersions prepared by ACC treatment with the ejection pressures of 100 and 200 MPa (left and right, respectively) at 10, 30, 60 and 90 Pass.

3.2. Helicity of collagen molecules after ACC treatment

Figure 5 shows the dependence of the CD spectra of aqueous collagen nanofiber dispersions on the Pass numbers when prepared by ACC at ejection pressures of 100 and 200 MPa. In CD spectroscopy, the transmitted light is supposed to alter the ellipsoidal polarization owing to different absorptivity against circular polarized light between the right and left sides. In measuring its CD spectra, a protein's secondary structure is eliminated. In this study, CD spectroscopy was employed to evaluate the molecular helicity in the higher structures of the collagen samples before and after the ACC treatment. To date, collagen has been reported to exhibit a unique CD spectrum in which a small positive peak appears at 220 nm, a crossover peaks appears near 213 nm and a large negative peak appears at ~197 nm [23, 24]; this spectrum has been also used as a reference to determine the presence of triple helices in collagen supramolecules. The Rpn value, which denotes the ratio of the positive peak over the negative peak in a CD spectrum, was also employed as a useful parameter to measure triple helical conformation. Typically, more than 0.1 for the Rpn indicates the presence of triple helices [25]. In this study, a negative and positive peak at 197 and 222 nm, respectively, appeared more or less in the CD spectra from both nanofibers of the CNF100 and CNF10 prepared by ACC treatment with ejection pressures of 100 and 200 MPa, respectively. Therefore, the obtained two collagen nanofibers were still considered to possess similar helices. The calculated Rpns in the CD spectra for all of the ACC-treated samples were greater than 0.1. This suggested that the left-handed, threefold, helical conformation of the collagen molecules in the initial fiber was maintained during ACC treatments, irrespective of the two different ejection pressures. Moreover, the intensities of the positive and negative peaks in the CD spectra of CNF100 at 100 MPa did not change significantly with the Pass numbers, whereas the corresponding intensities for CNF10 at 200 MPa increased with the increasing Pass number using the same sample collagen concentration. Previously, the ellipticity values of the collagen molecules at 220 nm have been reported to have a linear relationship with the collagen concentration [26]. Thus, decreases in the positive 220 nm maximum were assumed to reflect the disruption of the triple-fold helices. Therefore, the increasing ellipticity value with the Pass number assumed no degradation of the triple helices and further indicated increases in the

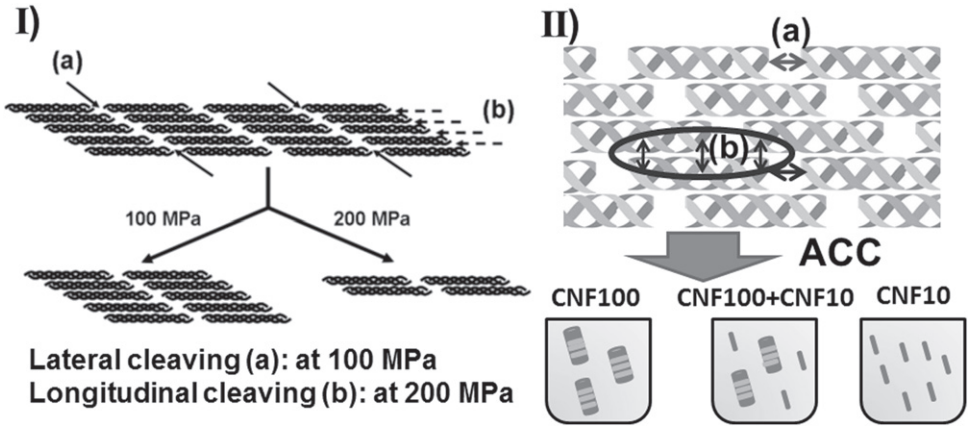

Figure 6. Possible cleavage patterns of a collagen fiber by ACC treatment, depending on the ejection pressure. Scheme I. Cleaving at either 100 or 200 MPa ejection pressure; (a) Lateral cleavage at 100 MPa and/or (b) Longitudinal cleavage at 200 MPa. Scheme II. Medial collision at a pressure between 100 and 200 MPa, which is a possible explanation why the resulting collagen nanofibers typically contained one of the two types, either CNF100 and/or CNF10, due to two critical interactions and/or lateral native crosslinks.

collagen supramolecules or in similar molecular structures as a result of the ACC method. This was suggested the conclusion that ACC treatment peeled off not only CNF10 having 10 nm in width from CNF100 surfaces but also collagen supramolecules, to some extent, into the resulting aqueous suspension with increasing in Pass number. In contrast, an ACC ejection pressure of 100 MPa was not sufficient to peel off the collagen supramolecules, but it could cleave intermolecular interactions in the lateral direction of the fibrils.

3.3. Pulverizing behavior on a collagen fiber by ACC treatments

A schematic model of the pulverizing behavior on a collagen fiber during ACC treatments is depicted in figure 6. The ACC treatment that used lower pressure water jets cleaved only the lateral molecular interactions (figures 6(I) and (a)), whereas the ACC at higher pressure cleaved both the longitudinal and lateral collagen fiber interactions (figures 6(I), (a) and (b)). The characteristic morphology of a collagen fibril, which is exhibited in the TEM images, was maintained after the ACC treatment at the lower pressure. However, the triple collagen helices were never cleaved to produce single polypeptides. In this manner, changing the ACC water jet pressure selectively cleaved specific interactions in the collagen fibers without the deformation of the component molecular triple helices. Therefore, when collagen fibers and fibrils were subjected to ACC treatments at various ejection pressures from 100–200 MPa, the resulting dispersions contained either only CNF100, CNF10 or a mixture of the two without a gradient change in the fiber width (figure 6(II)).

3.4. Tensile strength of single collagen nanofibers via sonication-induced fragmentation

The tensile strength of single collagen nanofibers was estimated using sonication-induced fragmentation [27–29]. This method, based on the fragmentation of nanofibers under hydrodynamic stresses caused by sonication-induced cavitation, has been applied to various

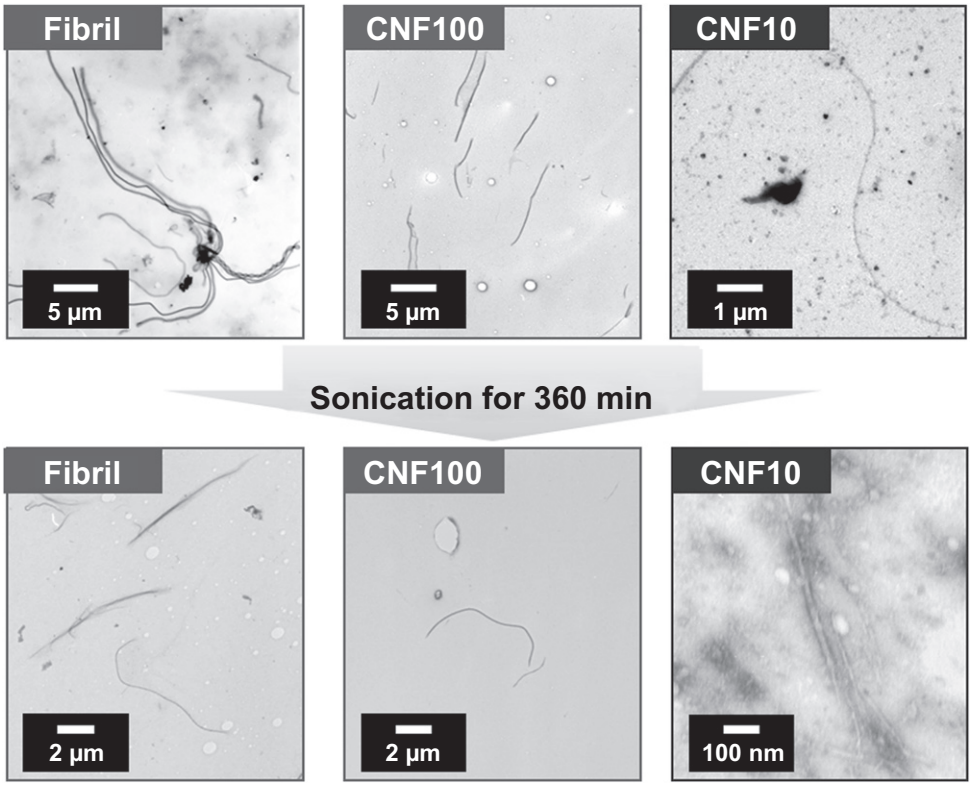

Figure 7. TEM images of collagen fibrils CNF100 and CNF10 before and after 360 min of sonication.

nanofibers, including carbon nanotubes, protein fibers and metal nanowires in aqueous systems [29]. In this method, the implosion dynamics of cavitation bubbles were induced by sonic wave propagation followed by radial solvent flow into cavity bubble centers. Then, the fiber around the cavity bubble is pulled into the bubble center, resulting in breakage from the tensile stress in the fiber. Tensile stress decreases as filaments become shorter, such that the tensile stress is no longer great enough to break the fiber. With prolonged sonication treatment, the fiber lengths were found to approach an almost constant value, which was concluded to be the limiting length (L_{lim}). Then, the tensile strength, which depends on the aspect ratio of the fragmented nanofibers, was estimated from the L_{lim}, to be described later.

3.4.1. Length and width of fragmented collagen nanofibers. The TEM images of the fragmented samples were observed in terms of the sonication time-course for collagen fibrils CNF100 and CNF10 (figure 7). Before sonication, the fibril lengths were distributed in a range from several μm to 30 μm. After a 60 min sonication, the lengths over 20 μm were decreased. Following further sonication for up to 360 min, the lengths of collagen fibrils CNF100 and CNF10 converged to certain ranges (figure 8). The length distributions were almost unchanged by additional sonication for longer than 360 min. Each length distribution range became narrower than it had been before the sonication. These results indicated that the fiber strength and tensile stress achieved equilibrium states after 360 min of sonication.

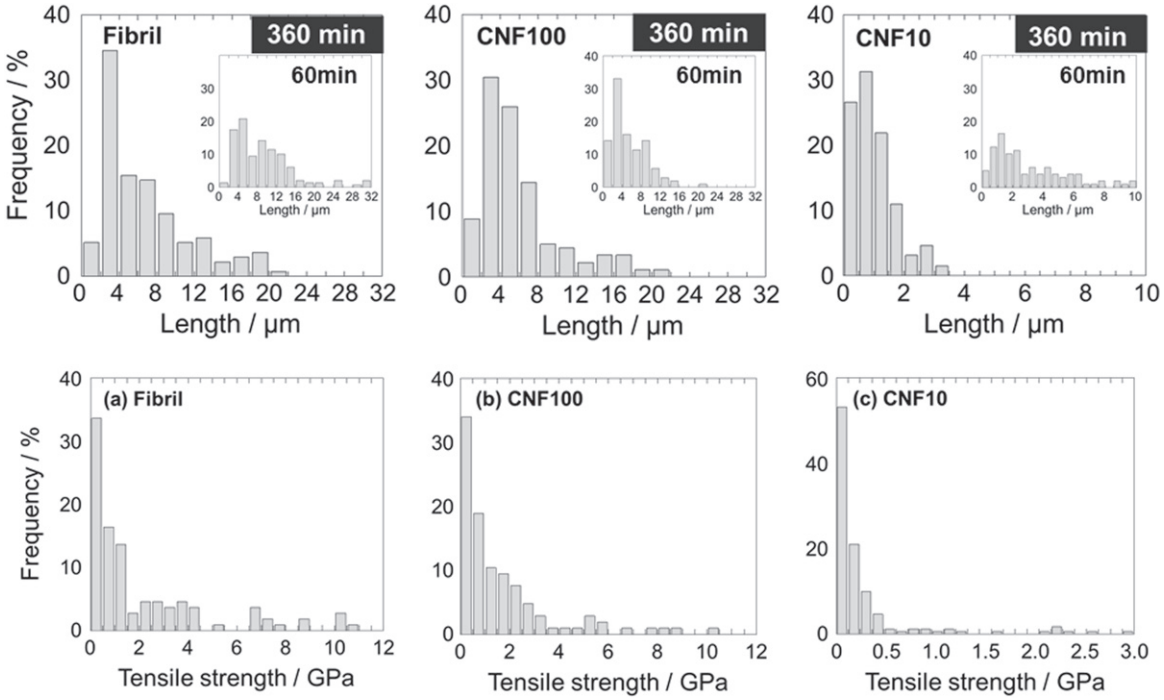

Figure 8. Length distribution of collagen fibrils CNF100 and CNF10 after 360 min of sonication. The insets show the results for the nanofibrils sonicated for 60 min. The strength of the (a) collagen fibrils, (b) CNF100 and (c) CNF10 are calculated by substituting the lengths and widths of 360 min-sonicated nanofibrils into equation (1). The lengths and widths of nanofibrils were measured from TEM images, shown in figure 7.

3.4.2. Tensile strength estimation of single collagen nanofibers. The tensile strength σ^* of the collagen nanofibers was estimated from the widths and lengths of fibers sonicated for 360 min using equation (1)

$$\sigma^* \approx 2 \times 10^5 \left(L_{\lim}/d\right)^2, \tag{1}$$

where σ^* is the fiber tensile strength, $L_{\lim}$ the limiting fiber length after sonication and d is the fiber width. Figures 8(a)–(c) exhibit the tensile strength distributions for the collagen fibrils, the CNF100 and the CNF10, respectively. In all of the fibers, the tensile strengths were widely distributed. In particular, the tensile strength for fibrils and for the CNF100 ranged from MPa to GPa, resulting in 1–3 GPa as the mean values, which corresponded to the tensile strengths for the wood and tunicate cellulose nanofibrils [28]. In contrast, the mean tensile strength for CNF10 was ~200 MPa. Moreover, Young's modulus was estimated to be ten times the tensile strength by giving consideration to a theoretical assumption regarding the defects of the packed hierarchical assembly in the collagen fibrils with staggered arrangements of supramolecules [30].

Here, it should be added that the sonication employed in the present study introduced mechanical defects in the collagen nanofibrils, including kinks. Such defects might have initiated catastrophic tensile fracturing, which is a dominant mechanism in sonication-induced fragmentation, and possibly lowered the inherent strength of the resulting nanofibrils.

3.4.3. Hierarchical structures of collagen fiber versus mechanical properties. As described above, the two types of collagen nanofibers prepared using ACC exhibited different tensile strengths; the tensile strength of CNF100 was about ten times higher than CNF10, indicating that greater numbers or amounts of lateral intermolecular interactions, including native crosslinks, could have contributed to the CNF100's higher tensile strength. It might be that the presence and amounts of the native crosslinks were critical factors for increasing tensile strength. As collagen fibrils are stabilized by longitudinal and lateral intermolecular interactions and crosslinks [31, 32], ACC treatment appeared capable of selectively cleaving intermolecular interactions in collagen fibrils, depending on the water ejection pressures (figure 6). ACC treatment at a 100 MPa ejection pressure cleaved mostly longitudinal intermolecular interactions in the collagen fibrils, whereas ACC treatment at 200 MPa cleaved both longitudinal and lateral intermolecular interactions. The results obtained thus far in this study suggested that the lateral intermolecular interactions, including the native crosslinks, could have been more strongly engaged than the intermolecular interactions in the longitudinal direction (figure 6(II)).

More specifically, the major intermolecular interactions and/or crosslinks that make up CNF10 were likely stronger since they are interactions that could not be cleaved by ACC. Namely, the collagen fibrils, the CNF100 and the CNF10 contained different intermolecular interactions, including native crosslinks in the lateral direction, which resulted in different tensile strengths. In a previous study, the reported tensile strength of the regenerated collagen fibrils from supramolecular solutions were lower than the results obtained in this study [33]. This different result was presumably because such regenerated collagen fibrils possessed no crosslinking, as they were already decomposed when the supramolecular solution was prepared from collagen fibrils. Conversely, the ACC method as a top-down process for native collagen fibers could not cleave the existing crosslinking, which thus persisted and resulted in tensile strengths higher than those observed in the regenerated fibrils. The two types of collagen nanofibers prepared using ACC exhibited different tensile strengths; the tensile strength of CNF100 was about ten times higher than CNF10. This indicates that greater numbers or amounts of lateral intermolecular interactions, including native crosslinks, could have contributed to the CNF100's higher tensile strength. It might be that the presence and amounts of the native crosslinks were critical factors for increasing the tensile strength.

In fibrils and in CNF100 after 360 min of sonication, the cleaving sites were found to be fibrillated (figure 9). In the TEM images of these sites, thinner fibers that were ~10 nm in width and similar to CNF10 were observed. In other words, the fibrous morphology of CNF10 remained after sonication. The result suggested the conclusion that some lateral intermolecular interactions that make up the collagen fibrils and CNF100 were selectively cleaved by sonication. However, the lateral intermolecular interactions and/or native crosslinking that make up CNF10 were strong enough to resist cleavage by sonication; thus, CNF10 might represent a critical minimum nanofibril unit.

3.5. Aqueous dispersion states of collagen nanofibers with different morphologies

As described previously, the ACC treatment at 100 MPa ejection pressure yielded short nanofibers, called CNF100, that had initial widths of ~100 nm as well as inherent periodic banding; this was in contrast to CNF10, which had one tenth the width at 10 nm after the ACC treatment at 200 MPa. Viscoelastic measurements were performed to examine the dispersion

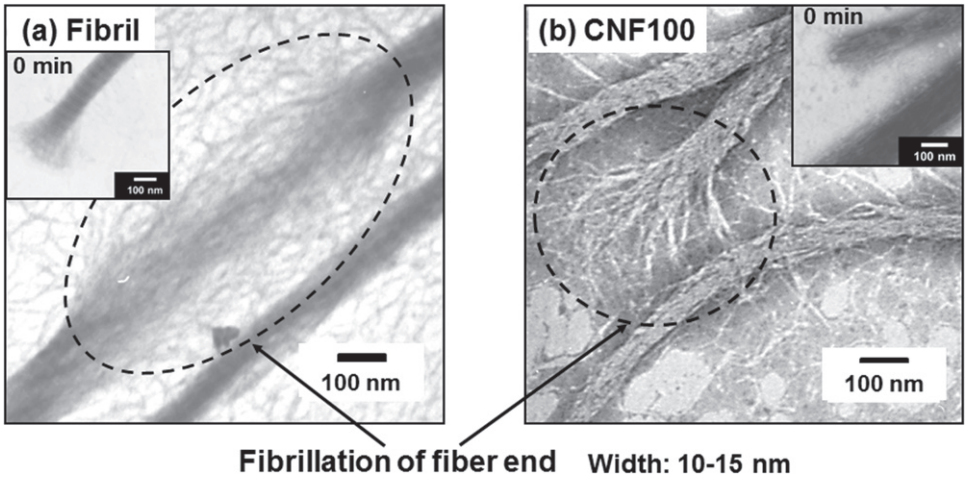

Figure 9. TEM images of just fibrillating (a) collagen fibrils and (b) CNF100 after 360 min of sonication, together with individual initial samples (insets) prior to sonication.

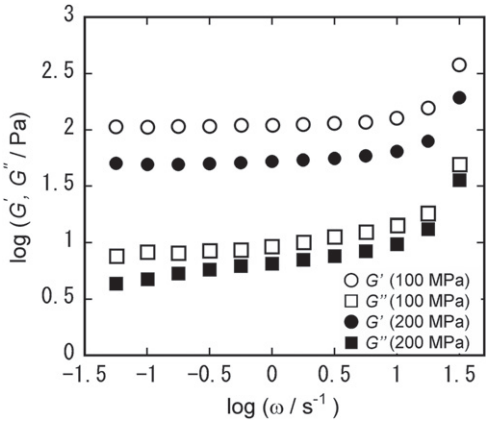

Figure 10. Dynamic storage modulus G' and loss modulus G'' versus the angular frequency for two different methods involving ACC treatment with a 30 Pass at ejection pressures of 100 and 200 MPa. The collagen concentration was 0.8% (by wt).

states of these two different systems using 100 and 200 MPa. Figure 10 shows the frequency dependence of the dynamic storage modulus, G', and loss modulus, G'', for the two resulting aqueous nanofiber dispersions. The G' and G'' values for the CNF100 dispersion were higher than those for the CNF10 dispersion. The G' and G'' of the aqueous fiber dispersions could be normally enhanced with increased crosslinkage points. In fact, a reduction in the width in the nanofibers resulted in increases in the specific surface areas, called a 'size effect'. In the present study, the aqueous dispersion of CNF100, which possesses a wider width, was supposed to have less contact among the fibers. However, this product exhibited higher G' and G'' values compared with the CNF10 dispersion with a lesser width. This observation, which did not agree with the above presumption, possibly was seen not because such a size effect was a dominant factor in the higher G' and G'' of the viscoelasticity but because of the greater mechanical strength of the wider periodic-banded CNF100. In addition, both the CNF100 and CNF10

aqueous dispersions were found in our study to exhibit gel formation at reduced temperatures of less than 4 °C. These remarkable nanofiber gel formations will be reported in a future paper.

4. Conclusions

Two types of separate collagen nanofibers distinguished by different widths were successfully prepared from native collagen fibers using the ACC. The widths of the prepared collagen nanofibers were independent of the ACC water jet ejection pressures (100–200 MPa). Specifically, 100 nm wide CNF100 was prepared under milder conditions than the 150 MPa ejection pressure, whereas 10 nm wide CNF10 was prepared mainly at over 150 MPa. Moreover, the triple helices in the collagen molecules remained intact after the ACC treatment.

The two types of collagen nanofibers prepared using ACC exhibited different tensile strengths; the tensile strength of CNF100 was about ten times higher than that of CNF10. In addition, collagen nanofibers might have different mechanical properties in the lateral direction as well as the axial direction. A nano-indentation method using atomic force microscopy has demonstrated the lateral elasticity of the collagen nanofibers [34, 35]. A previous study has shown that the mechanical strength of the molecular scaffold affects cell differentiation [36, 37]. Therefore, the two collagen nanofibers prepared here by ACC have the potential for controlling cell differentiation in possibly different ways, as they have different mechanical properties. This encourages the consideration of the application of CNF100 and CNF10 in the fabrication of new functional materials with unique properties such as a scaffold for tissue engineering.

CNF100, which has a wider width, exhibited the higher viscoelasticity in aqueous dispersion when compared with the lesser width of CNF10. This is contrary to the general sense of nanosize effects in fibers. Namely, the morphology of the periodic-banded CNF100 was likely to be a dominant factor that contributed to its viscoelasticity. More detailed research is required regarding this aspect of these substances.

Acknowledgments

The authors thank Dr Shunji Hattori, Nippi Inc., Tokyo, Japan for kindly providing the collagen sample and Mr Kichiro Kondo at Japan Spectroscopy Corporation (JASCO), Tokyo, Japan for his measurements of the circular dichroic (CD) spectra.

References

[1] Emons A M C and Mulder B M 2000 How the deposition of cellulose microfibrils builds cell wall architecture *Trends. Plant. Sci.* **5** 35–40

[2] Silver F H, Freeman J W and Seehra G P 2003 Collagen self-assembly and the development of tendon mechanical properties *J. Biomech.* **36** 1529–53

[3] Persikov A V, Ramshaw J A, Kirkpatrick A and Brodsky B 2000 Amino acid propensities for the collagen triple helix *Biochemistry* **39** 14960–7

[4] Meyers M A, Chen P Y, Lin A Y M and Seki Y 2008 Biological materials: structure and mechanical properties *Progr. Mater. Sci.* **53** 1–206

[5] Trus B L and Piez K A 1980 Compressed microfibril models of the native collagen fibril *Nature* **286** 300–1

[6] Chen J M, Kung C E, Feairheller S H and Brown E M 1991 An energetic evaluation of a 'Smith' collagen microfibril model *J. Protein. Chem.* **10** 535–52

[7] Bailey A J, Robins S P and Balian G 1974 Biological significance of the intermolecular crosslinks of collagen *Nature* **251** 105–9
[8] Kadler K E, Holmes D F, Trotter J A and Chapman J A 1996 Collagen fibril formation *Biochem. J.* **316** 1–11
[9] Schmitt F O, Hall C E and Jakus M A 1942 Electron microscope investigation of the structure of collagen *J. Cell. Comp. Physiol.* **20** 11–33
[10] Petruska J A and Hodge A J 1964 A subunit model for the tropocollagen macromolecule *Proc. Natl. Acad. Sci. USA* **51** 871–6
[11] Christiansen D L, Huang E K and Silver F H 2000 Assembly of type I collagen: fusion of fibril subunits and the influence of fibril diameter on mechanical properties *Matrix. Biol.* **19** 409–20
[12] Roeder B A, Kokini K, Sturgis J E, Robinson J P and Voytik-Harbin S L 2002 Tensile mechanical properties of three-dimensional type I collagen extracellular matrices with varied microstructure *J. Biomech. Eng.* **124** 214–22
[13] Kessler A, Rosen H and Levenson S M 1960 Chromatographic fractionation of acetic acid-solubilized rat tail tendon collagen *J. Biol. Chem.* **235** 989–94
[14] Yoshimura K, Terashima M, Hozan D and Shirai K 2000 Preparation and dynamic viscoelasticity characterization of alkali-solubilized collagen from shark skin *J. Agric. Food Chem.* **48** 685–90
[15] Flory P J and Garrett R R 1958 Phase transitions in collagen and gelatin systems *J. Am. Chem. Soc.* **80** 4836–45
[16] Kondo T, Morita M, Hayakawa K and Onda Y 2008 Wet pulverizing of polysaccharide *US Patent* 7,357,339
[17] Kondo T, Kose R, Naito H and Kasai W 2014 Aqueous counter collision using paired water jets as a novel means of preparing bio-nanofibers *Carbohydr. Polym.* **112** 284–90
[18] Kose R, Mitani I, Kasai W and Kondo T 2011 'Nanocellulose' as a single nanofiber prepared from pellicle secreted by *Gluconacetobacter xylinus* using aqueous counter collision *Biomacromolecules* **12** 716–20
[19] Tsuboi K, Yokota S and Kondo T 2014 Difference between bamboo- and wood-derived cellulose nanofibers prepared by the aqueous counter collision method *Nord. Pulp paper Res. J.* **29** 69–76
[20] Kose R and Kondo T 2013 Size effects of cellulose nanofibers for enhancing the crystallization of poly(lactic acid) *J. Appl. Polym. Sci.* **128** 1200–5
[21] Kawano Y and Kondo T 2014 Preparation of aqueous carbon material suspensions by aqueous counter collision *Chem. Lett.* **43** 483–5
[22] Zeng S, Zhang C, Lin H, Yang P, Hong P and Jiang Z 2009 Isolation and characterisation of acid-solubilised collagen from the skin of Nile tilapia (*Oreochromis niloticus*) *Food Chem.* **116** 879–83
[23] Brown F R III, Carver J P and Blout E R 1969 Low temperature circular dichroism of poly(glycyl-L-prolyl-L-alanine) *J. Mol. Biol.* **39** 307–13
[24] Brown F R III, di Corate A, Lorenzi G P and Blout E R 1972 Synthesis and structural studies of two collagen analogues: Poly(L-prolyl-L-seryl-glycyl) and poly(L-prolyl-L-alanyl-glycyl) *J. Mol. Biol.* **63** 85–99
[25] Kwak J, Capua A D, Locardi E and Goodman M 2002 TREN (Tris(2-aminoethyl)amine): an effective scaffold for the assembly of triple helical collagen mimetic structures *J. Am. Chem. Soc.* **124** 14085–91
[26] Chu F H and Lukton A 1974 Collagenase induced changes in the circular dichroism spectrum of collagen *Biopolymers* **13** 1427–34
[27] Ahir S V, Huang Y Y and Terentjev E M 2008 Polymers with aligned carbon nanotubes: active composite materials *Polymer* **49** 3841–54
[28] Saito T, Kuramae R, Wohlert J, Berglund L A and Isogai A 2013 An ultrastrong nanofibrillar biomaterial: the strength of single cellulose nanofibrils revealed via sonication-induced fragmentation *Biomacromolecules* **14** 248–53
[29] Huang Y Y, Knowles T P J and Terentjev E M 2009 Strength of nanotubes, filaments, and nanowires from sonication-induced scission *Adv. Mater.* **21** 3945–8
[30] Young R J and Lovell P A 1981 *Introduction to polymers* 2nd edn (Boca Raton FL: CRC Press) pp 319–21
[31] Kang A H and Gross J 1970 Relationship between the intra and intermolecular cross-links of collagen *Proc. Natl. Acad. Sci. USA* **67** 1307–14

[32] Streeter I and de Leeuw N H 2011 A molecular dynamics study of the interprotein interactions in collagen fibrils *Soft Matter* **7** 3373–82
[33] van der Rijt J A, van der Welf K O, Bennink M L, Dijkstra P J and Feijen J 2007 Micromechanical testing of individual collagen fibrils *Macromol. Biosci.* **18** 697–702
[34] Wenger M P E, Bozec L, Horton M A and Mesquida P 2007 Mechanical properties of collagen fibrils *Biophys. J.* **93** 1255–63
[35] Strasser S, Zink A, Janko M, Heckl W M and Thalhammer S 2007 Structural investigations on native collagen type I fibrils using AFM *Biochem. Biophys. Res. Commun.* **354** 27–32
[36] Engler A J, Sen S, Sweeney H L and Discher D E 2006 Matrix elasticity directs stem cell lineage specification *Cell* **126** 677–89
[37] McDaniel D P, Shaw G A, Elliott J T, Bhadriraju K, Meuse C, Chung K H and Plant A L 2007 The stiffness of collagen fibrils influences vascular smooth muscle cell phenotype *Biophys. J.* **92** 1759–69